Human Multipotent Mesenchymal Stromal Cells in the Treatment of Postoperative Temporal Bone Defect: An Animal Model

Lukas Skoloudik, Viktor Chrobok, David Kalfert, Zuzana Koci, Eva Sykova, Tetyana Chumak, Jiri Popelar, Josef Syka, Jan Laco, Jana Dedková, et al.

Cell Transplantation, Vol. 25, pp. 1405–1414, 2016

0963-6897/16 $90.00 + .00
DOI: http://dx.doi.org/10.3727/096368915X689730
E-ISSN 1555-3892
www.cognizantcommunication.com

Human Multipotent Mesenchymal Stromal Cells in the Treatment of Postoperative Temporal Bone Defect: An Animal Model

Lukas Skoloudik,* Viktor Chrobok,* David Kalfert,* Zuzana Koci,†‡§ Eva Sykova,†‡ Tetyana Chumak,† Jiri Popelar,† Josef Syka,† Jan Laco,¶ Jana Dedková,# Govindan Dayanithi,†**††‡‡ and Stanislav Filip§§

*Department of Otorhinolaryngology and Head and Neck Surgery, University Hospital Hradec Kralové, Charles University in Prague, Faculty of Medicine in Hradec Kralové, Hradec Kralové, Czech Republic
†Institute of Experimental Medicine, Czech Academy of Sciences, Prague, Czech Republic
‡Department of Neuroscience, 2nd Faculty of Medicine, Charles University in Prague, Prague, Czech Republic
§Bioinova, Ltd., Prague, Czech Republic
¶The Fingerland Department of Pathology, University Hospital Hradec Kralové, Charles University in Prague, Faculty of Medicine in Hradec Kralové, Hradec Kralové, Czech Republic
#Department of Radiology, University Hospital Hradec Kralové, Charles University in Prague, Faculty of Medicine in Hradec Kralové, Hradec Kralové, Czech Republic
**Department of Molecular Neurophysiology, Institute of Experimental Medicine, Czech Academy of Sciences, Prague, Czech Republic
††Institut National de la Santé et de la Recherche Médicale, Unité de recherche U1198, Université Montpellier, Montpellier, France
‡‡Ecole Pratique des Hautes Etudes-Sorbonne, Paris, France
§§Department of Oncology and Radiotherapy, Charles University in Prague, Faculty of Medicine in Hradec Kralové, Hradec Kralové, Czech Republic

Canal wall down mastoidectomy is one of the most effective treatments for cholesteatoma. However, it results in anatomical changes in the external and middle ear with a negative impact on the patient's quality of life. To provide complete closure of the mastoid cavity and normalize the anatomy of the middle and external ear, we used human multipotent mesenchymal stromal cells (hMSCs), GMP grade, in a guinea pig model. A method for preparing a biomaterial composed of hMSCs, hydroxyapatite, and tissue glue was developed. Animals from the treated group were implanted with biomaterial composed of hydroxyapatite and hMSCs, while animals in the control group received hydroxyapatite alone. When compared to controls, the group implanted with hMSCs showed a significantly higher ratio of new bone formation ($p=0.00174$), as well as a significantly higher volume percentage of new immature bone ($p=0.00166$). Our results proved a beneficial effect of hMSCs on temporal bone formation and provided a promising tool to improve the quality of life of patients after canal wall down mastoidectomy by hMSC implantation.

Key words: Temporal bone; Middle ear surgery; Human bone marrow; Human mesenchymal stromal cells (hMSCs); Guinea pig model; Transplantation; Osteogenesis

INTRODUCTION

In addition to harboring hematopoietic stem cells, the bone marrow compartment also harbors nonhematopoietic stem cells, the most noteworthy of which are multipotent mesenchymal stromal cells (MSCs) (16). MSCs are multipotent progenitor cells of stromal origin, which have also been found in various other tissues, such as adipose tissue, umbilical cord blood, Wharton's jelly, placenta, dental pulp, skin, heart, and spleen (11,23). During the last decade, the properties of MSCs have been extensively investigated and applied for regenerative purposes. Such special interest has been triggered by their self-renewal and multilineage differentiational capacity. MSCs differentiate into various tissues of mesodermal origin, including osteocytes, chondrocytes, adipocytes (11,23), fibroblasts, and smooth muscle cells (14). Isolation of MSCs is usually performed by their adherence to plastic, which enables their ex vivo cultivation to reach large

Received June 25, 2015; final acceptance February 10, 2016. Online prepub date: October 22, 2015.
Address correspondence to Prof. Stanislav Filip, M.D., Ph.D., D.Sc., Department of Oncology and Radiotherapy, Charles University in Prague, Faculty of Medicine in Hradec Kralové, Hradec Kralové, Czech Republic. Tel: +420 495 834 618; E-mail: filip@fnhk.cz

numbers. Dominici et al. (3) defined MSCs by their negative expression of hematopoietic surface markers (CD34, CD14, CD45) and simultaneous expression of adhesive molecules (CD44, CD39, CD105, CD73, CD166). MSCs have been reported to home to areas of tissue injury and participate in tissue repair (11). The regeneration processes of MSCs can be performed by direct differentiation or indirectly via the secretion of a variety of growth factors and cytokines that exert a paracrine, protective effect on ischemic cells (8) by stimulating angiogenesis, limiting inflammation, suppressing apoptosis, and recruiting tissue-specific progenitor cells (19). Currently, it is thought that the indirect effects of MSCs are especially responsible for their therapeutic potential (1,8). This has led to their use in clinical applications requiring bone (31) and cartilage replacement, repair of tissue after acute myocardial infarction, renal failure, stroke (24), critical limb ischemia (4,12), or neurological conditions (30).

Bone replacement in otorhinolaryngology is used for skeletal reconstruction of injured bone, postoperative bone deficit, or treatment of congenital abnormalities. MSC transplantation is an alternative to extensive plastic surgery using autologous bone grafts or vascularized flap reconstruction. MSCs have been explored to avoid complications associated with harvesting bone and decrease morbidity of both the donor and recipient. MSCs can be directly injected into the fracture sites to facilitate healing. In the case of bone reconstruction, MSCs are compounded with an osteoconductive biomaterial. Ceramic-based graft substitute materials include calcium sulfate-based materials, such as hydroxyapatite, β-tricalcium phosphate, and bioactive glass. Cultured MSCs on scaffolds in osteogenic media induce bone development de novo (9).

Otolaryngologists focus on MSC research as a great tool for the regeneration of injured tissue or replacement of missing tissue after surgery. Temporal bone reconstruction after middle ear surgery is still considered a problem for otologists. The management of middle ear cholesteatoma occasionally requires a canal wall down (CWD) mastoidectomy. This approach is very effective in cholesteatoma treatment, as it reduces the recurrence rate of cholesteatoma to as low as 2% (27). Unfortunately, the CWD technique changes the anatomy of the external and middle ear. The ear canal loses its self-clearing ability, and the exteriorized mastoid cavity becomes a target for chronic infections. Patients need regular treatment with bathing restrictions and hearing aid limitations. Some of the cavity problems have been reduced using the obliteration technique (2,7,15,29). The obliteration of mastoid cavity only reduces the size of the cavity. Currently, no surgical technique provides complete closure of the mastoid cavity and normalization of the anatomy of the middle and external ear.

The considerable potential of MSCs for the regeneration and replacement of bone tissue has generated great interest among otologists (10,28). Due to advances in the field of tissue engineering, biomaterials, and cell biology, MSCs may play an important role in the regeneration of the temporal bone. However, there is a lack of evidence concerning the efficacy of MSCs to replace bone in a specific location such as the middle and external ear. New bone formation should keep up the function and aeration of the middle ear cavity. Inflammatory changes in the small tympanic cavity or changes in the inner ear could deteriorate hearing. For that reason, effective MSC treatment should focus not only on anatomical and histological changes in the bone alone but also the anatomical and histological changes of the surrounding soft tissue and inner ear. Therefore, the purpose of this study was set to evaluate the effect of hMSCs on the reconstruction of a postoperative temporal bone defect in a guinea pig model. Clinical evaluation included animal survival, clinical signs of inflammatory changes, and exploration of tympanic bula. Radiological evaluation focused on closing the bone defect, determining the density of the new bone formation, as well as aeration of the middle ear, changes of middle ear mucosa, and radiologic changes of the inner ear. Histopathological evaluation consisted of standard histological examination, and immunohistochemical examination focused on osteogenesis, angiogenesis, and inflammatory changes. The comparison of the treated group with the control group (osteogenic scaffold without MSCs) enabled the effect of hMSCs to be distinguished.

MATERIALS AND METHODS

Animals

Twenty adult male guinea pigs (weight 240–410 g) were used for this study, and they were purchased from Lubos Sobota farm (Mestec Kralove, Czech Republic, license No. 28177/2009/17210) and were quarantined for 2 weeks prior to the experiments. The animals were housed individually with access to food and fresh water available ad libitum. Animal care procedures were carried out according to the European Community Council and Czech Republic Directives guidelines (#86/609/EEC), and experiments were performed with the approval of the Institutional Ethical Committee of Charles University in Prague, Medical Faculty in Hradec Králové (authorization # 4/2013). All animals had normal eardrums without middle ear discharge.

Experimental Design

Four animals were used to introduce the surgical approach and optimize the implantation of the biomaterial. Other animals were randomly divided into experimental ($n=8$) and control groups ($n=8$). In the experimental group, the biomaterial combined with hMSCs in third

passage (suspension of autologous MSC 3P in 1.5 ml; Bioinova, Ltd., Prague, Czech Republic) was implanted (Fig. 1A). Control group animals were implanted with the biomaterial alone (Fig. 1B). After the surgery, all animals were given an immunosuppressive treatment of cyclosporine A (CSA; Novartis, Munich, Germany) at a dose of 10 mg/kg per day. At day 30 after the surgery, animals were sacrificed by intraperitoneal injection of 100 mg/kg of ketamine hydrochloride (Gedeon-Richter, Budapest, Hungary) and 10 mg/kg of xylazine hydrochloride (Interchemie Gasternory, Adelaar, Holland) and transcardially perfused with 10% formaldehyde (Sigma-Aldrich, St. Louis, MO, USA). The results were evaluated by Equal-Variance T-Test (software NCSS 9; NCSS, LLC, Kaysville, UT, USA). The statistical analysis was performed by a certified statistician.

Surgery

The guinea pigs were anesthetized with an intramuscular injection of 50 mg/kg ketamine hydrochloride (Gedeon-Richter) and 5 mg/kg xylazine hydrochloride (Interchemie Gasternory). An anterior surgical approach to the left tympanic bulla was chosen. After submandibular skin incision, the anterior surface of the tympanic bulla was exposed. The hole, 4 mm in diameter, was made using a microdissector and small forceps. The hole was covered with the biomaterial (Fig. 2). The wound was closed with a single layer of 3-0 Safil suture. Carprofen (Janssen Pharmaceutica NV, CCPC, Beerse, Belgium) was used as an analgesic at a dose of 4 mg/kg, and enrofloxacine (eBioscience, San Diego, CA, USA) was used at a dose of 10 mg/kg. Both were applied intramuscularly at the end of the surgery.

Cell Preparation

All procedures connected with the cell isolation, expansion, and preparation were conducted by Bioinova, Ltd. Bone marrow was aspired into a collection kit (Bioinova, Ltd.) from the iliac crest of healthy donors after informed consent was obtained. In summary, bone marrow was applied on Gelofusine® (B. Braun, Melsungen AG, Germany), and the mononuclear fraction was collected and used for cultivation. The mononuclear fraction was seeded on plastic flasks (70,000–140,000 cells/cm^2; TPP Techno Plastic Products AG, Trasadingen, Switzerland) and allowed to adhere. Nonadherent cells were removed after 24 and 48 h by replacing the media. Adherent cells were cultured at 37°C in a humidified atmosphere containing 5% CO_2 in enriched α-MEM (Lonza Inc., Walkersville, MD, USA) containing platelet lysate (5%; Bioinova, Ltd.) and gentamicin (10 μg/ml; Gentamicin Lek®; Lek Pharmaceuticals, Ljubljana, Slovenia). The media was changed twice a week. According to their spindle-shaped morphology and plastic adherence, the cells were identified as MSCs. After reaching near confluence, cells were harvested by a TrypLE™ (Life Technologies, Carlsbad, CA, USA) and were then passaged and seeded again onto a fresh plastic surface. Cells were harvested in the third passage, 4 weeks after the initial seeding. Cells were counted and analyzed for surface markers (Fig. 3A), microbiological contamination, and sterility. Several batches of the product were

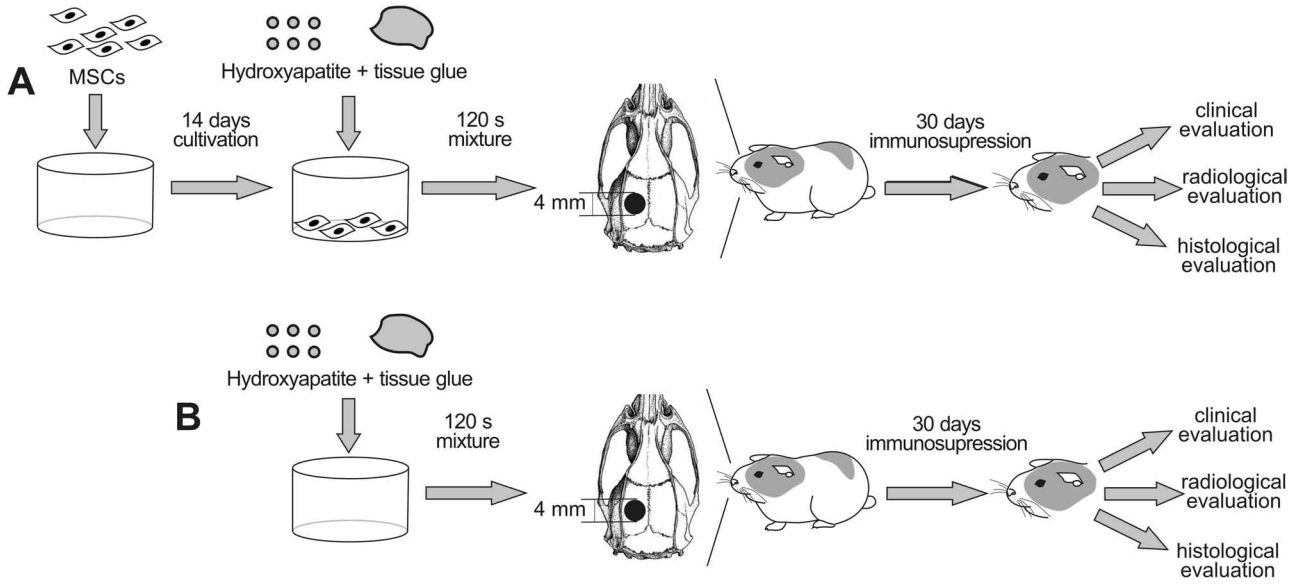

Figure 1. Schematic diagram of the experimental protocol. Implantation of biomaterial with MSCs into the bone defect of a guinea pig in the experimental group (A) and implantation of the scaffold without MSCs in the control group (B).

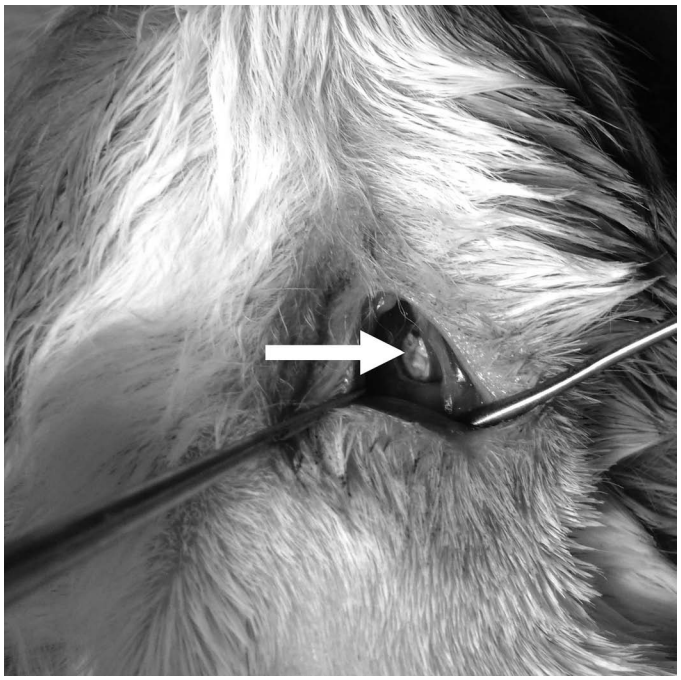

Figure 2. Photograph showing the operation of the left tympanic bulla. Arrow shows the implantation of the biomaterial with MSCs into the bony defect of the tympanic bulla.

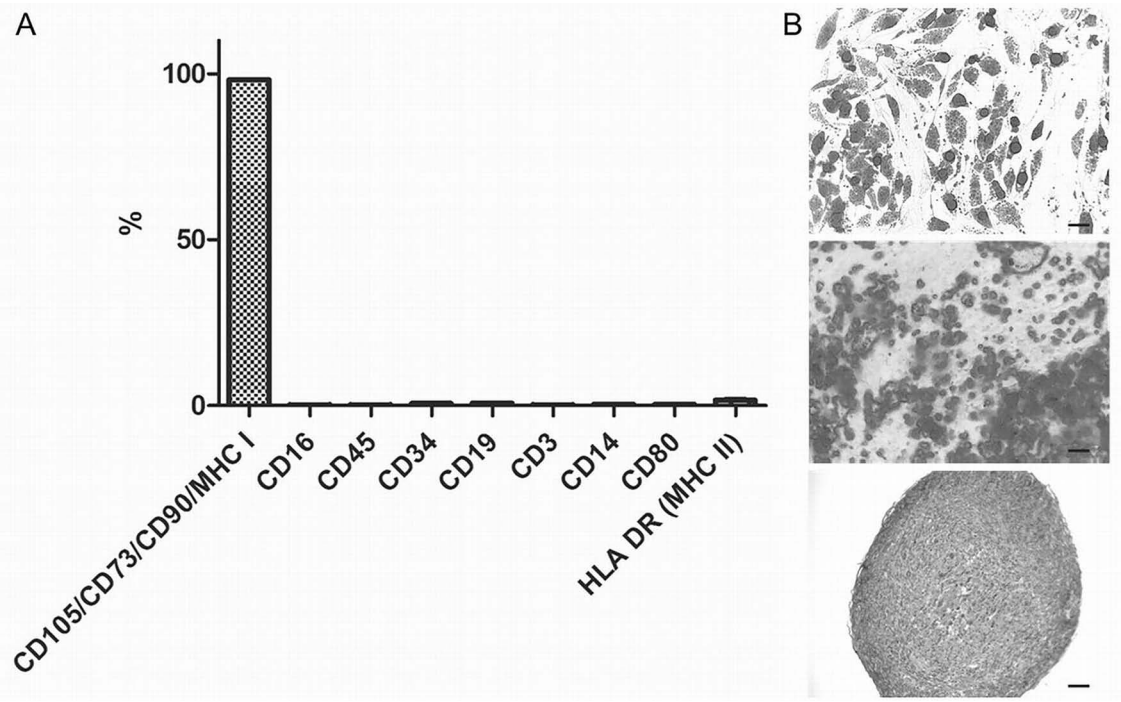

Figure 3. Analysis of surface markers and characteristics of administered product. The suspension of autologous MSC 3P was analyzed and certified by Bioinova, Ltd., for the expression of MSC surface markers and surface markers of possible contaminating cells (A), and tested for multipotent differentiation capacity (B). In vitro differentiation into adipocytes (B top, scale bar: 100 μm), osteoblasts (B middle, scale bar: 100 μm), and chondrocytes (B bottom, scale bar: 50 μm).

tested for MSC multilineage potential to differentiate into adipogenic, osteogenic, and chondrogenic cell linages (Fig. 3B). The cell suspension containing 20×10^6 of autologous MSCs was released for implantation.

Scaffold Preparation

Hydroxyapatite (Cem-Ostetic™; Berkeley Advanced Biomaterials, Berkeley, CA, USA) was used to fill the bone defect and provide MSCs with a sufficient scaffold. Thanks to its chemical similarity [Ca_{10} (PO_4)$_6$ (OH)$_2$] to organic bone, the material has excellent biocompatibility and osteoconductive potential. Hydroxyapatite has proved to be a good scaffold for osteogenic cell populations; 1 cm^3 of synthetic bone graft was powdered, and 100 mg was combined with tissue glue (Tisseel Lyo, Baxter Czech, Prague, Czech Republic) and seeded with 1.6×10^6 MSCs. An appropriate piece of scaffold that suited the created bone defect was used for each osteogenic implant. Implants without MSCs were used for the control group.

Radiological Evaluation

Radiological examination was performed using 128-row multidetector Computed Tomography (CT; Siemens SOMATOM Definition AS/AS+), with an HRCT (high-resolution computed tomography) reconstruction algorithm. Source data collimation was 0.625 mm, table feed was 4 mm/s, coronal plane reconstructions were obtained, slice thickness 0.4 mm, FOV 55×55 mm, matrix 512×512, images were evaluated in window center 700 HU and window width 4000 HU.

Histopathological Evaluation

The temporal bone specimens were fixed in 10% neutral formalin (Sigma-Aldrich) for 24 h and then gently decalcified using 5% formic acid (Sigma-Aldrich) for 5 days. After sectioning, the tissue was embedded in paraffin, cut into 4-μm-thick slices, and stained with hematoxylin (Sigma-Aldrich) and eosin (Junsei Chemicals, Tokyo, Japan) (H&E) and Masson's trichrome (MT; Sigma-Aldrich). In addition, each case was stained for chloroacetate esterase (CHAE; Sigma-Aldrich) according to standard histochemical procedure.

For immunohistochemical examination, 4-μm-thick sections were cut from paraffin blocks, mounted on slides coated with 3-aminopropyltriethoxy-silane, deparaffinized in xylene, and rehydrated in descending grades (100–70%) of ethanol (all reagents: Sigma-Aldrich). Indirect immunohistochemistry was performed using monoclonal or polyclonal antibodies against CD3 (polyclonal, 1:200), CD20 (L26, 1:300), CD31 (JC70A, 1:50), CD68 (PG-M1, 1:50), and tartrate-resistant acid phosphatase (TRAP) (ab58008, 1:750). All antibodies were purchased from Dako (Glostrup, Denmark), except for TRAP (Abcam, Cambridge, UK). The staining for TRAP was done manually. For antigen retrieval, the tissue was processed in the microwave vacuum histoprocessor RHS 1 (Milestone, Sorisole, Italy) at pH 6.0 at 97°C for 4 min. Endogenous peroxidase activity was inhibited by immersing the sections in 3% hydrogen peroxide (MT; Sigma-Aldrich). After incubation with the antibody, the sections were subjected to EnVision+ Dual Link System-HRP (Dako). Finally, the reaction was visualized using 3-3′-diaminobenzidine (DAB) (Sigma-Aldrich), and the slides were counterstained with H&E. The staining of all remaining antibodies was performed using immunostainer BenchMark Ultra (Roche, Basel, Switzerland), with Ultra View Universal DAB Detection Kit and Bluing Reagent as the visualization reagent and chromogen (all reagents: Roche).

All specimens were evaluated by a blinded pathologist (J.L.). The zone with the implanted material was examined for an inflammatory response, as well as for angiogenesis and new bone formation under a light microscope (Olympus, Prague, Czech Republic). Specifically, the numbers of CHAE$^+$ neutrophils, eosinophils, CD3$^+$ T lymphocytes, and CD20$^+$ B lymphocytes in three high-power fields (HPFs) (10× eyepiece and 40× objective; area 0.152 mm^2) were counted in the areas in which the inflammation was most intense. The presence of CD68$^+$ and TRAP$^+$ macrophages was also examined. Angiogenesis was assessed in so-called "hot spots" based on the number of small blood vessel lumina depicted by CD31$^+$ endothelial cells, using a 20× objective (area 0.283 mm^2) (18). Using NIS Elements AR 3.0 program, new bone formation was calculated as the ratio (total area of new formed bone trabeculae)/(total area of the implantation zone).

Any pathological changes of middle ear and inner ear structures were also recorded.

Statistical Analysis

Data are presented as mean and standard deviation. The results were statistically evaluated by means of equal variance *t*-test. A value of $p<0.05$ was considered to be significant. All data were analyzed by NCSS 9.

RESULTS

Clinical Evaluation

At the completion of the study, 30 days after surgery, seven out of eight animals from the control group and eight out of eight animals from the experimental group were available for evaluation. One animal from the control group died as a result of operative trauma. In all other animals, wound healing was achieved without any complications. No signs of otitis media or postoperative vestibulopathy were present. Macroscopic exploration of the tympanic bulla proved firm occlusion of the operative defect in the anterior wall of the bulla in all cases (Fig. 4). No inflammatory response occurred around the site of the implanted material.

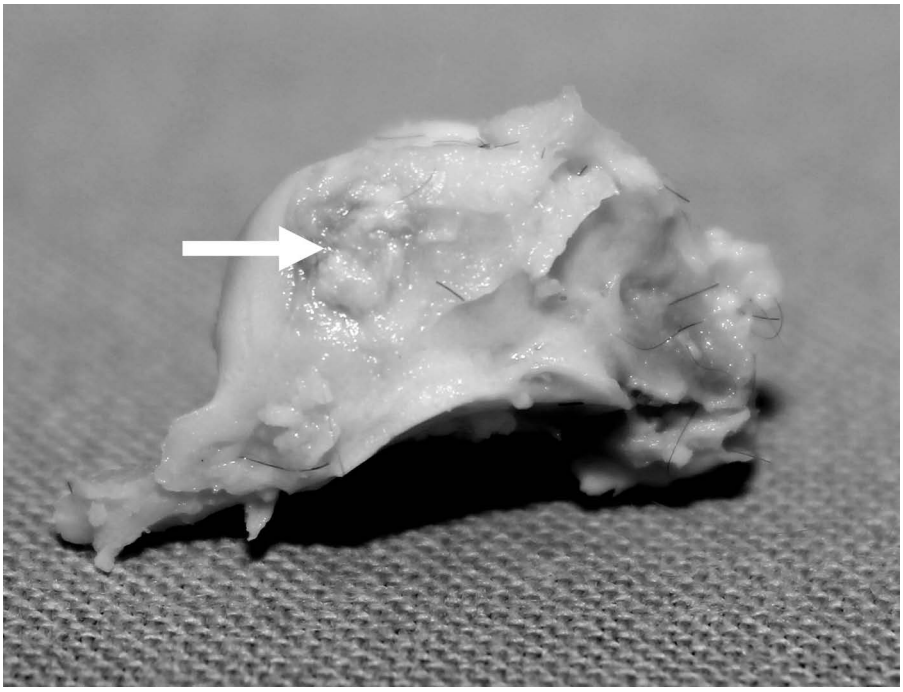

Figure 4. Image of the tympanic bulla 30 days after implantation. Arrow shows the osteointegration of the biomaterial with MSCs.

Radiological Evaluation

Using HRCT, we evaluated the maximal bone density and areal bone density hot spots in the site of the implanted material, inflammatory signs in the tympanic bulla with thickness of the middle ear mucosa, aeration of the tympanic bulla, effusion in the middle ear, and changes in the inner ear (Fig. 5).

The bone density hot spots of implanted material with MSCs were 800 HU to 1,100 HU, with a mean density of 980 HU. In the control group, bone density hot spots were 920 HU to 1,300 HU, with a mean density of 1,050 HU ($p = 0.225$). The areal bone densities in the experimental group were 540 HU to 800 HU, with a mean density of 720 HU. In the control group, the areal densities were 630 HU to 850 HU, with a mean density of 780 HU ($p = 0.201$). Both density and areal density hot spots were significantly different in both groups (Table 1).

The thickening of the middle ear mucosa was observed in only a few animals (one experimental and three controls), and this difference was nonsignificant ($p = 0.282$). All animals had an aerial tympanic bulla without effusion in the middle ear. In both groups, the CT scan did not show any pathological changes in the inner ear.

Histopathological Evaluation

Osteogenesis. In all 15 temporal bones, the pathologist identified the zone of implanted material. Osteogenesis was observed in both groups (Fig. 6). In the experimental group, the mean ratio of new bone formation was 616,846 μm² and median 622,089 μm² in 1 mm² of implanted material. In the control group, we observed osteogenesis at a lower rate. The mean ratio of new bone formation was 227,470 μm², median 289,369 μm², in 1 mm² of implanted material. This difference was highly significant ($p = 0.00174$). The volume percentage of new immature bone in the temporal bone defect was 62% in the experimental group when compared to 23% in the control group. This difference was also highly significant ($p = 0.00166$).

Angiogenesis. Angiogenesis was observed in both groups. In the experimental group, the mean number of small blood vessel lumina (depicted by $CD31^+$ endothelial cells) was 13 in an area of 0.283 mm^2, and the median was 13. In the control group the mean number of blood vessels was eight with a median of seven. Statistical evaluation revealed that the difference was not significant (95% confidence interval; $p = 0.08092$).

Inflammation

Immunohistochemically, it was proven that $CD3^+$ T lymphocytes were present in both groups of temporal bones. In the experimental group, the mean number of $CD3^+$ T lymphocytes was 65, with a median of 65. In the control group, the mean number was 24 with a median of 19. The difference was statistically significant ($p = 0.00368$). $TRAP^+$ cells of the macrophage lineage were noted in all specimens. Immunohistochemical

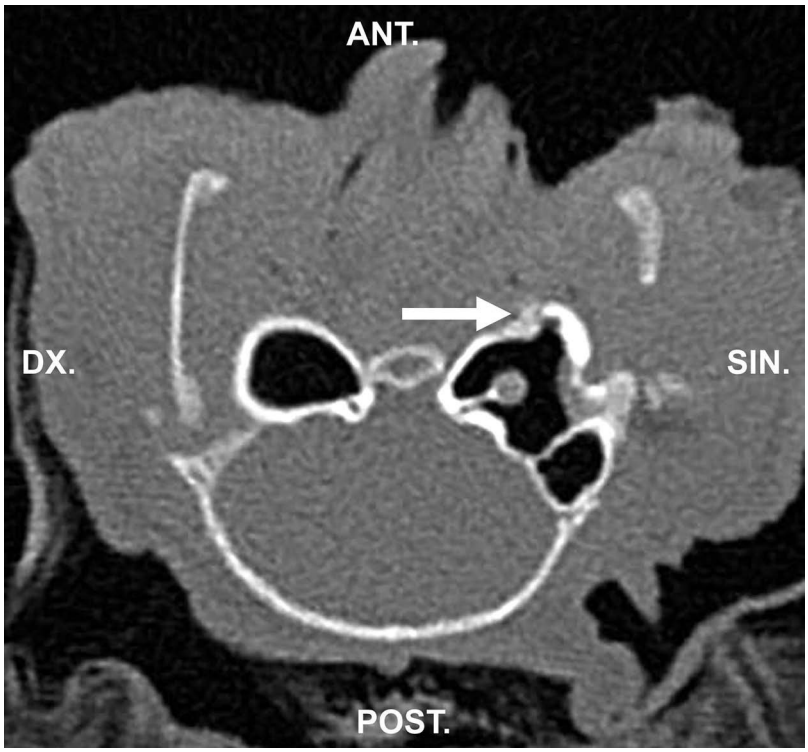

Figure 5. Radiological examination by HRCT of guinea pig head, level of tympanic bulla, 30 days after implantation of biomaterial with MSCs. Arrow shows the place of the implanted biomaterial into the bone defect.

analysis revealed no CHAE$^+$ neutrophils, CD20$^+$ B lymphocytes, or CD68$^+$ cells (Table 2).

Histology of Inner Ear

In all 15 specimens, histological examination of the cochlea showed vital neuroepithelium without any abnormalities in the inner ear.

DISCUSSION

Reconstruction of complex craniofacial deformities is a clinical challenge in situations of injury, congenital defects, or disease. The use of cell-based therapies represents one of the most advanced methods for enhancing the regenerative response for craniofacial wound healing. Both somatic and stem cells have been adopted in the treatment of complex osseous defects, and advances have been made in finding the most adequate scaffold for the delivery of cell therapies in human regenerative medicine (22).

Healing and regenerative processes are associated with inflammation (5) where humoral factors interact together with cells and the microenvironment (6). Inflammation is shown to play an important role in fracture repair, particularly during the initial and remodeling phases of healing. However, chronic exposures to lymphocytes and to inflammatory signaling have been shown to impair the fracture repair process (13,17). For example, in the bone repair process, macrophages and monocytes, which are distributed as osteoclasts at the injury site, play a key role. It has been demonstrated that the absence of B cells does not compromise the normal osteoblast distribution connected with bone growth and healing through intramembranous ossification and that the B cells have a minimal effect or, at the most, cause redundancy of osteoblast function during the modeling of bone (25). These findings support the notion that it is necessary to ascertain the presence of certain inflammatory markers and thereby

Table 1. HRCT of Guinea Pig Temporal Bone: Density of Implanted Biomaterial

	Experimental Group			Control Group			Statistical
	Minimal	Maximal	Mean	Minimal	Maximal	Mean	Significance
Hot spot density	800	1,100	980	920	1,300	1,050	$p=0.225$
Areal density	540	800	720	630	850	780	$p=0.201$

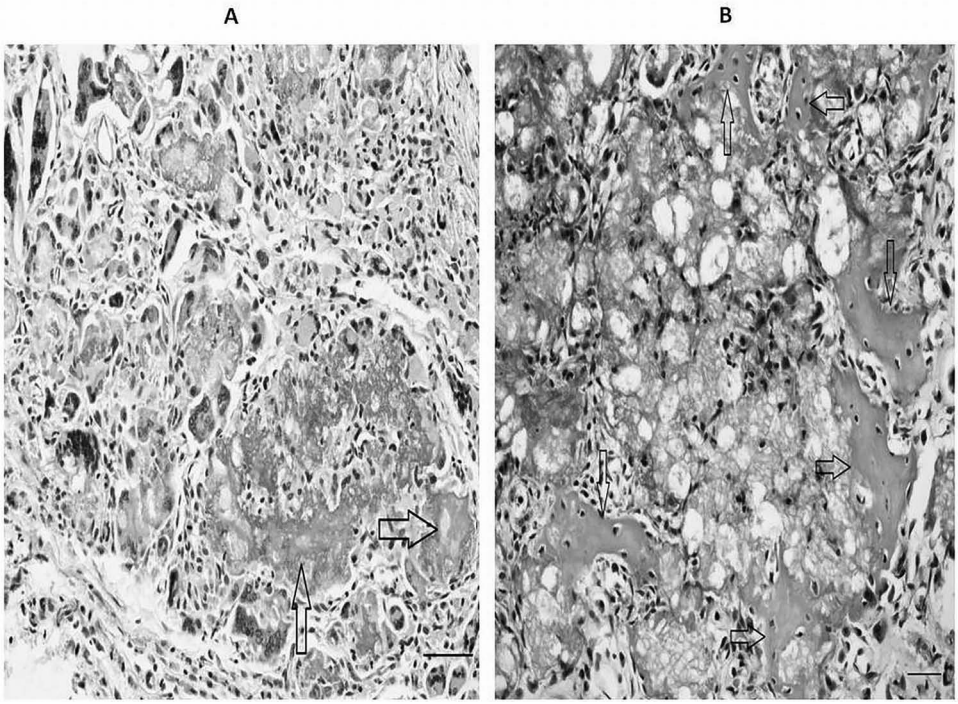

Figure 6. Histological microscopic examination in the implantation or control zone. Newly formed bone trabeculae (black arrows) are in direct contact with hydroxyapatite (seen as a bubbly grayish material). The amount of osteoid between control sample (A) and sample with MSCs (B) were estimated and compared. H&E. Scale bars: 100 μM.

distinguish the actual degree of inflammation and the repair process (20).

In our study, immunohistochemical examination revealed a significantly higher distribution of $CD3^+$ T lymphocytes in the experimental group. We also observed $TRAP^+$ cells, which is indicative of cells of a macrophage lineage, in all specimens. Migration of T lymphocytes and macrophages could be the paracrine effect of MSCs that leads to facilitation of osteogenesis. MSCs have a potential to directly or indirectly inhibit or activate certain immune cells and thus affect the overall response of the body to tissue injury and repair processes (11).

An adverse inflammatory response of neutrophils could damage the implanted material and bone reconstruction. In our experiments, we did not detect a distribution of $CHAE^+$ cells (neutrophils). The absence of an adverse inflammatory response confirms our findings and HRCT scan of the tympanic bulla. Macroscopic exploration of the tympanic bulla confirmed the firm occlusion of the operative defect in the anterior wall of the bulla in all cases. No inflammatory response occurred around the site of the implanted material or in the middle ear. It is known that middle ear infection manifests by middle ear secretion. In our experiments, the CT scan showed the aerial tympanic bulla without any secretion. Furthermore, the indirect marker of middle ear inflammation is the thickness of the middle ear mucosa, and this thickness was unchanged in the majority of the animals tested (six out

Table 2. Histopathological Evaluation of Guinea Pig Temporal Bone

	Experimental Group (Mean Ratio)	Control Group (Mean Ratio)	Statistical Significance
New bone formation (μm² in 1 mm²)	616,846	227,470	$p=0.00174$
New bone formation (volume %)	62	23	$p=0.00166$
Angiogenesis ($CD31^+$ cells in 0.283 mm^2)	13	8	$p=0.08092$
$CD3^+$ T lymphocytes (in 0.152 mm^2)	65	24	$p=0.00368$
$CHAE^+$ neutrophils	0	0	
$CD20^+$ B lymphocytes	0	0	
$CD68^+$ cells	0	0	
$TRAP^+$ macrophages	Positive in all cases	Positive in all cases	

of seven and five out of eight in the control and experimental groups, respectively).

Recent investigations [see review by Pacini and Petrini (21)] have made considerable progress in the understanding of tissue regeneration driven by MSCs. Recent data also indicated the anatomical location of MSCs as residing in the "perivascular" space of blood vessels dispersed throughout the whole body. This histological localization suggested that MSCs contribute to the formation of new blood vessels in vivo. MSCs have also been shown to release angiogenic factors and protease to facilitate blood vessel formation and are able to promote/support angiogenesis in vitro (21). However, the lack of vessels alone does not ensure sufficient nutritional support of the bone graft (26) and is responsible for the failure in many bone repair applications. Early vascularization driven by the angiogenic effect of MSCs could ensure an ingrowth of osteogenic reparative cells into a composite in a critical bone defect. Indeed, in our experiment, we detected angiogenesis so-called "hot spots" as small blood vessel lumina depicted by $CD31^+$ endothelial cells.

In our study, we evaluated new blood vessels immunohistochemically by CD31 staining for endothelial cells, and the results revealed a significantly higher number of small blood vessels in the experimental group constituting biomaterial of the MSCs. Although the median of small vessels in the experimental group was almost two times higher (13 vs. 7 in area of 0.283 mm^2), the difference was less significant ($p = 0.08$).

Reconstruction of complex craniofacial deformities is a clinical challenge in situations of injury, congenital defects, or disease. The use of cell-based therapies represents one of the most advanced methods for enhancing the regenerative response for craniofacial wound healing. Both somatic and stem cells have been adopted in the treatment of complex osseous defects, and advances have been made in finding the most adequate scaffold for the delivery of cell therapies in human regenerative medicine. We evaluated the effect of MSCs in the reconstruction of postoperative temporal bone defect. Compared to other bone defect locations, the middle ear has some nuance. We reconstructed the new bone between the cavity and soft tissue, and the shape and position of the newly formed bone was achieved, as shown by HRCT scan followed by an exploration of the tympanic bulla. The anatomical result of MSC implantation was satisfactory. The newly formed bone closed the tympanic bulla and appeared to be the proper shape without any known abnormalities. To elucidate the effect of MSCs, we compared osteoneogenesis in a biomaterial with and without MSCs. We observed a significantly higher degree of osteoneogenesis in the experimental group with MSC implantation. Together, the present results confirm the positive effects of hMSCs on temporal bone reconstruction in a guinea pig model.

ACKNOWLEDGMENTS: This work was supported by MH CZ-DRO (UHHK, 00179906), by the program PRVOUK P37/06, P37/11 (LF UK), and NPU of MEYS (LO1309). The authors wish to thank Dr. Eva Cermakova for statistical analysis. Govindan Dayanithi belongs to the Centre National de la Recherche Scientifique–The Ministry of Research and Higher Education–Paris, France. We are very grateful to Elisa Brann, IEM AS CR, for her critical reading of the manuscript. The authors declare no conflicts of interest.

REFERENCES

1. Bortolotti, F.; Ukovich, L.; Razban, V.; Martinelli, V.; Ruozi, G.; Pelos, B.; Dore, F.; Giacca, M.; Zaschigna, S. In vivo therapeutic potential of mesenchymal stromal cells depends on the source and the isolation procedure. Stem Cell Rep. 4:332–339; 2015.
2. Cheney, M. L.; Megerian, C. A.; Brown, M. T.; McKenna, M. J.; Nado, J. B. The use of the temporoparietal fascial flap in temporal bone reconstruction. Am. J. Otol. 17:137–142; 1996.
3. Dominici, M.; Le Blanc, K.; Mueller, I.; Slaper-Cortenbach, I.; Marini, F.; Krause, D.; Deans, R.; Keating, A.; Prockop, D. J.; Horwitz, E. Minimal criteria for defining multipotent mesenchymal stromal cells. The International Society for Cellular Therapy position statement. Cytotherapy 8:315–317; 2006.
4. Dubský, M.; Jirkovská, A.; Bem, R.; Fejfarova, V.; Varga, M.; Kolesar, L.; Pagacova, L.; Sykova, E.; Jude, E. B. Role of serum levels of angiogenic cytokines in assessment of angiogenesis after stem cell therapy of diabetic patients with critical limb ischemia. Cell Transplant. 23:1517–1523; 2014.
5. Ekström, K.; Omar, O.; Granéli, C.; Wang, X.; Vazirisani, F.; Thomsen, P. Monocytes exosomes stimulate the osteogenic gene expression of mesenchymal stem cells. PLoS One 8:e75227; 2013.
6. Forbes, S. J.; Rosenthal, N. Preparing the ground for tissue regeneration: From mechanism to therapy. Nat. Med. 20:857–869; 2014.
7. Franco-Vidal, V.; Daculsi, G.; Bagot d'Arc, M.; Sterkers, O.; Smail, M.; Robier, A.; Bordure, P.; Claros, P.; Paiva, A.; Darrouzet, V.; Anthoine, E.; Bebear, J. P. Tolerance and osteointegration of TricOs(TM)/MBCP(®) in association with fibrin sealant in mastoid obliteration after canal wall-down technique for cholesteatoma. Acta Otolaryngol. 134:358–366; 2014.
8. Gnecchi, M.; Danieli, P.; Cervio, E. Mesenchymal stem cell therapy for heart disease. Vascul. Pharmacol. 57:48–55; 2012.
9. He, J.; Genetos, D. C.; Leach, J. K. Osteogenesis and trophic factor secretion are influenced by the composition of hydroxyapatite/poly(lactide-co-glycolide) composite scaffolds. Tissue Eng. Part A 16:127–137; 2010.
10. Jang, C. H.; Park, H.; Cho, Y. B.; Song, C. H. Mastoid obliteration using a hyaluronic acid gel to deliver a mesenchymal stem cells-loaded demineralized bone matrix: An experimental study. Int. J. Pediatr. Otorhinolaryngol. 72:1627–1632; 2008.
11. Kaplan, J. M.; Youd, M. E.; Lodie, T. A. Immunomodulatory activity of mesenchymal stem cells. Curr. Stem Cell Res. Ther. 6:297–316; 2011.
12. Kočí, Z.; Turnovcová, K.; Dubský, M.; Baranovičová, L.; Holáň, V.; Chudíčková, M.; Syková, E.; Kubinová, Š. Characterization of human adipose tissue-derived stromal

cells isolated from diabetic patient's distal limbs with critical ischemia. Cell Biochem. Funct. 32:597–604; 2014.
13. Kovach, T. K.; Dighe, A. S.; Lobo, P. I.; Cui, Q. Interactions between MSCs and immune cells: Implications for bone healing. J. Immunol. Res. 2015:752510; 2015.
14. Kurisaki, A.; Ito, Y.; Onuma, Y.; Intoh, A.; Asashima, M. In vitro organogenesis using multipotent cells. Hum. Cell 23:1–14; 2010.
15. Leatherman, B. D.; Dornhoffer, J. L. Bioactive glass ceramic particles as an alternative for mastoid obliteration: Results in an animal model. Otol. Neurol. 23:657–660; 2002.
16. Mendez-Ferrer, S.; Michurina, T. V.; Ferrari, F.; Mazloom, A. R.; Macarthur, B. D.; Lira, S. A.; Scadden, D. T.; Ma´ayan, A.; Enikopolov, G. N.; and Frenette, P. S. Mesenchymal and hematopoietic stem cells from a unique bone marrow niche. Nature 466:829–834; 2010.
17. Miron, V. E.; Franklin, R. J. Macrophages and CNS remyelination. J. Neurochem. 130: 165–171; 2014.
18. Murray, B.; Wilson, D. J. A study of metabolites as intermediate effectors in angiogenesis. Angiogenesis 4:71–77; 2001.
19. Murray, I. R.; West, C.; Hardy, W. R.; James, A. W.; Park, T. S.; Nguyen, A.; Tawonsawatruk, T.; Lazzari, L.; Soo, C.; Péault, B. Natural history of mesenchymal stem cells, from vessel walls to culture vessels. Cell. Mol. Life Sci. 71:1353–1374; 2014.
20. Oryan, A.; Monazzah, S.; Bigham-Sadegh, A. Bone injury and fracture healing biology. Biomed. Environ. Sci. 28:57–71; 2015.
21. Pacini, S.; Petrini, I. Are MSCs angiogenic cells? New insights on human nestin-positive bone marrow-derived multipotent cells. Front. Cell Dev. Biol. 2:20; eCollection 2014.
22. Pagni, G.; Kaigler, D.; Rasperini, G.; Avila-Ortiz, G.; Bartel, R.; Goannobile, W. V. Bone repair cells for craniofacial regeneration. Adv. Drug Deliv. Rev. 64:1310–1319; 2012.
23. Pittenger, M. F.; Mackay, A. M.; Beck, S. C.; Jaiswal, R. K.; Douglas, R.; Mosca, J. D.; Moorman, M. A.; Simonetti, D. W.; Craig, S.; Marshak, D. R. Multilineage potential of adult human mesenchymal stem cells. Science 284:143–147; 1999.
24. Potier, E.; Noailly, J.; Ito, K. Directing bone marrow-derived stromal cell function with mechanics. J. Biochem. 43:807–814; 2010.
25. Raggatt, L. J.; Alexander, K. A.; Kaur, S.; Wu, A. C.; Mac Donald, K. P.; Pettit, A. R. Absence of B cells doses not compromise intramembranous bone formation during healing in a tibial injury model. Am. J. Pathol. 182:1501–1508; 2013.
26. Seebach, C.; Henrich, D.; Wilhelm, K.; Barker, J. H.; Marzi, I. Endothelial progenitor cells improve directly and indirectly early vascularization of mesenchymal stem cell-derived bone regeneration in a critical bone defect in rats. Cell Transplant. 21:1667–1677; 2012.
27. Shohet, J. A.; da Jong, A. L. The management of pediatric cholesteatoma. Otolaryngol. Clin. North Am. 35:841–851; 2002.
28. Skoloudik, L.; Chrobok, V.; Kalfert, D.; Koci, Z.; Filip, S. Multipotent mesenchymal stromal cells in otorhinolaryngology. Med. Hypotheses 82:769–773; 2014.
29. Suzuki, H.; Ikezaki, S.; Imazato, K.; Koizumi, H.; Ohbuchi, T.; Hohchi, N.; Hashida, K. Partial mastoid obliteration combined with soft-wall reconstruction for modele ear cholesteatoma. Ann. Otol. Rhinol. Laryngol. 123:571–575; 2014.
30. Syková, E.; Forostyak, S. Stem cells in regenerative medicine. Laser Ther. 2287–2292; 2013.
31. Vaněček. V.; Klíma, K.; Kohout, A.; Foltán, R.; Jiroušek, O.; Šedý, J.; Štulík, J.; Syková, E.; Jendelová, P. The combination of mesenchymal stem cells and a bone scaffold in the treatment of vertebral body defects. Eur. Spine J. 22:2777–2786; 2013.